DALTON
FULL PAPER

Manganese(III) *meso*-tetrakis(*ortho*-*N*-alkylpyridyl)porphyrins. Synthesis, characterization, and catalysis of $O_2^{\bullet -}$ dismutation †

Ines Batinić-Haberle,*[a] Ivan Spasojević,[a] Robert. D. Stevens,[b] Peter Hambright[c] and Irwin Fridovich[a]

[a] *Department of Biochemistry, Duke University Medical Center, Durham, NC 27710, USA. E-mail: ines@chem.duke.edu*
[b] *Department of Pediatrics, Duke University Medical Center, Durham, NC 27710, USA*
[c] *Department of Chemistry, Howard University, Washington, DC 20059, USA*

Received 28th January 2002, Accepted 3rd May 2002
First published as an Advance Article on the web 7th June 2002

A series of *ortho* isomers of *meso*-tetrakis(*N*-alkylpyridyl)porphyrins (alkyl being methyl, ethyl, n-propyl, n-butyl, n-hexyl, and n-octyl) and their Mn(III) complexes were synthesized and characterized by elemental analysis, uv/vis spectroscopy, electrospray ionization mass spectrometry and electrochemistry. An increase in the number of carbon atoms in the alkyl chains from 1 to 8 is accompanied by an increase in: (a) lipophilicity, as measured by the chromatographic retention factor, R_f; (b) metal-centered redox potential, $E_{1/2}$ from +220 to +367 mV *vs.* NHE, and (c) proton dissociation constant, pK_{a2} from 10.9 to 13.2. A linear correlation was found between $E_{1/2}$ and R_f of the Mn(III) porphyrins and between the pK_{a2} and R_f of the metal-free compounds. As the porphyrins become increasingly more lipophilic, the decrease in hydration disfavors the creation of charge, while enhancing the electron-withdrawing effect of the positively charged pyridyl nitrogen atoms. Consequently, $E_{1/2}$ increases linearly with the increase in pK_{a2}, a trend in porphyrin basicity opposite from the one we previously reported for other water-soluble Mn(III) porphyrins. All of these Mn(III) porphyrins are potent catalysts for superoxide dismutation (disproportionation). Despite the favorable increase of $E_{1/2}$ with the increase in chain length, the catalytic rate constant decreases from methyl (log k_{cat} = 7.79) to n-butyl, and then increases such that the n-octyl is as potent a SOD mimic as are the methyl and ethyl compounds. The observed behavior originates from an interplay of hydration and steric effects that modulate electronic effects.

Introduction

Low-molecular weight catalytic scavengers of reactive oxygen and nitrogen species, aimed at treating oxidative stress injuries, have been actively sought. Three major groups of manganese complexes have been developed and tested *in vitro* and *in vivo*; Mn porphyrins,[1–9] Mn cyclic polyamines[10] and Mn salen derivatives.[11] Based on structure–activity relationships that we developed for water-soluble Mn(III) and Fe(III) porphyrins,[2–4] Mn(III) *meso*-tetrakis(*N*-methylpyridinium-2-yl)porphyrin (Mn^{III}TM-2-PyP^{5+}, AEOL-10112) and *meso*-tetrakis(*N*-ethylpyridinium-2-yl)porphyrins (Mn^{III}TE-2-PyP^{5+}, AEOL-10113) were proposed and then shown to be potent catalysts for superoxide dismutation.[4,12] The alkyl substitutions at the *ortho* positions restrict the rotation of the pyridyl rings with respect to the porphyrin plane. Consequently both compounds exist as mixtures of four atropoisomers, all of which were shown to be equally potent catalysts for $O_2^{\bullet -}$ dismutation.[13] These Mn porphyrins also allow SOD-deficient *Escherichia coli* to grow under aerobic conditions,[4,12] and offer protection in rodent models of oxidative stress such as stroke,[14] diabetes,[15] sickle cell disease,[16] and cancer/radiation.[17] The high formal +5 charge of these metalloporphyrins could influence their tissue distribution, transport across biological membranes, and binding to other biomolecules and their low lipophilicities may restrict their protective effects. With the aim of modulating metalloporphyrin subcellular distribution, higher *N*-alkylpyridylporphyrin analogues (Scheme 1) with increased lipophilicity were synthesized. We anticipate that their comparative kinetic and thermodynamic characterization will deepen our insight into the modes of action of porphyrin-based catalytic antioxidants and the mechanisms of oxidative stress injuries.

† Electronic supplementary information (ESI) available: cyclic voltammetry and electrospray mass spectrometry plots. See http://www.rsc.org/suppdata/dt/b2/b201057g/

Experimental

Abbreviations

SOD, superoxide dismutase; AN, acetonitrile; DMF, *N*,*N*′-dimethylformamide; NHE, normal hydrogen electrode; TLC, thin-layer chromatography; H_2P^{4+}, any *meso*-tetrakis(*N*-alkylpyridyl)porphyrin ligand; $Mn^{III/II}P^{4+/5+}$, any Mn(III/II) *meso*-tetrakis(*N*-alkylpyridyl)porphyrin; *meso* refers to the substituents at the 5, 10, 15, and 20 (*meso* carbon) positions of the porphyrin core. Mn^{III}T(alkyl)-2(3,4)-PyP^{5+}, manganese(III) *meso*-tetrakis((*N*-methyl-, *N*-ethyl-, *N*-n-propyl-, *N*-n-butyl-, *N*-n-hexyl-, *N*-n-octyl-)pyridinium-2(3,4)-yl)porphyrin; alkyl is M, methyl; E, ethyl; nPr, n-propyl; nBu, n-butyl; nHex, n-hexyl; nOct, n-octyl on the pyridyl ring; 2 is the *ortho*, 3, the *meta* and 4 the *para* isomer; Mn^{III}TM-2-PyP^{5+} is AEOL-10112, and Mn^{III}TE-2-PyP^{5+} is AEOL-10113; Mn^{III}P-Tr(M-2-PyP^{4+}, manganese(III) 5-phenyl-10,15,20-tris(*N*-methylpyridinum-2-yl)porphyrin; Mn^{III}BM-2-PyP^{3+}, manganese(III) *meso*-bis(2-pyridyl)bis(*N*-methylpyridinium-2-yl)porphyrin; Mn^{III}TrM-2-PyP^{4+}, 5-(2-pyridyl)-10,15,20-tris(*N*-methylpyridinium-2-yl)porphyrin; Mn^{III}T(TMA)P^{5+}, manganese(III) *meso*-tetrakis(*N*,*N*,*N*-trimethylanilinium-4-yl)porphyrin; Mn^{III}T-(TFTMA)P^{5+}, manganese(III) *meso*-tetrakis(2,3,5,6-tetrafluoro-*N*,*N*,*N*-trimethylanilinium-4-yl)porphyrin; Mn^{III}TCPP^{3-}, manganese(III) *meso*-tetrakis(4-carboxylatophenyl)porphyrin; MnTSPP^{3-}, manganese(III) *meso*-tetrakis(4-sulfonatophenyl)-

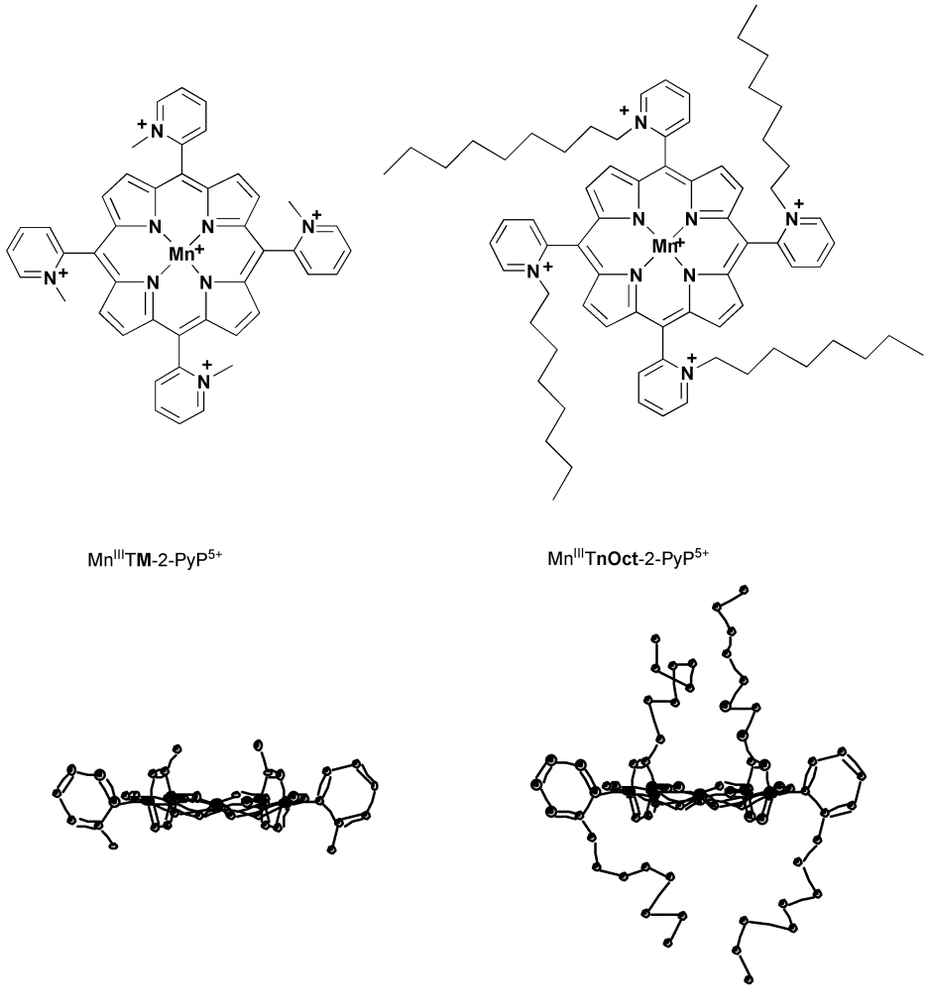

Scheme 1 Structures of the most hydrophilic ($Mn^{III}TM$-2-PyP^{5+}) and the most lipophilic ($Mn^{III}TnOct$-2-PyP^{5+}) members of the series studied. The αβαβ atropoisomers are shown.

porphyrin; $Mn^{III}T(2,6\text{-}Cl_2\text{-}3\text{-}SO_3\text{-}P)P^{3-}$, manganese(III) *meso*-tetrakis(2,6-dichloro-3-sulfonatophenyl)porphyrin; $Mn^{III}T(2,6\text{-}F_2\text{-}3\text{-}SO_3\text{-}P)P^{3-}$, manganese(III) *meso*-tetrakis(2,6-difluoro-3-sulfonatophenyl)porphyrin; $Mn^{III}T(2,4,6\text{-}Me_3\text{-}3,5\text{-}(SO_3)_2\text{-}P)P^{7-}$, manganese(III) *meso*-tetrakis(2,4,6-trimethyl-3,5-disulfonatophenyl)porphyrin; Mn^{III}hematoP^{-}, manganese(III) hematoporphyrin IX.

General

$MnCl_2{\cdot}4H_2O$, and Baker-flex silica gel IB TLC plates were purchased from J. T. Baker. *N*,*N*′-Dimethylformamide, ethyl *p*-toluenesulfonate, 2-propanol (99.5+%), NH_4PF_6 (99.99%), NaCl, sodium L-ascorbate (99+%) and tetrabutylammonium chloride were from Aldrich, while xanthine, and ferricytochrome c were from Sigma. The n-propyl, n-butyl, n-hexyl and n-octyl esters of *p*-toluenesulfonic acid were from TCI America. Methanol (anhydrous, absolute), ethanol (absolute), acetone, ethyl ether (anhydrous), chloroform, EDTA and KNO_3 were from Mallinckrodt and acetonitrile was from Fisher Scientific. Xanthine oxidase was prepared by R. Wiley and was supplied by K. V. Rajagopalan.[18] Catalase was from Boehringer, ultrapure argon from National Welders Supply Co., and tris buffer (ultrapure) was from ICN Biomedicals, Inc.

Synthesis

H_2T(alkyl)-2-PyP^{4+}. *Meso*-tetrakis(2-pyridyl)porphyrin, H_2T-2-PyP was purchased from Mid-Century Chemicals, Chicago, IL. The increased lipophilicity of the n-propyl, n-butyl, n-hexyl, and n-octyl analogues required a slight modification of the synthetic approach used for methyl and ethyl compounds.[4,12] Typically, to 100 mg of H_2T-2-PyP in 20 mL of DMF at 100 °C, was added 4 mL of the corresponding *p*-toluenesulfonate. The course of *N*-alkylation was followed by thin-layer chromatography on silica gel TLC plates using 1 : 1 : 8 KNO_3-saturated H_2O : H_2O : acetonitrile as a mobile phase. While complete *N*-alkylation is achieved within a few hours for the methyl analogue, the required time gradually increases and it took three and five days to prepare the n-hexyl and n-octyl compounds, respectively. Upon completion, for the methyl, ethyl and n-propyl compounds, the reaction mixture was poured into a separatory funnel containing 200 mL each of water and chloroform and shaken well. The chloroform layer was discarded and the extraction with $CHCl_3$ was repeated several times. The n-butyl, n-hexyl and n-octyl analogues are more lipophilic and tended to remain in the chloroform layer. Therefore, increasing amounts of methanol were added to the water/$CHCl_3$ mixture in order to force the porphyrin into the aqueous/methanol layer. This layer was filtered and the porphyrin was precipitated as the PF_6^- salt by the addition of a concentrated aqueous solution of NH_4PF_6. The precipitate was thoroughly washed with 1 : 1 2-propanol : diethyl ether in the case of methyl and ethyl compounds and with pure diethyl ether for the others. The dried precipitate was then dissolved in acetone, filtered and precipitated as the chloride salt by the addition of tetrabutylammonium chloride dissolved in acetone. The precipitate was washed thoroughly with acetone, and dried *in vacuo* at room temperature. Elemental analysis: H_2TnPr-2-$PyPCl_4{\cdot}12.5H_2O$ ($C_{52}H_{71}N_8O_{12.5}Cl_4$): Found: C, 54.2; H, 6.42; N, 9.91; Cl, 12.04. Calculated: C, 54.20; H, 6.18; N, 9.68; Cl, 12.25%. H_2TnBut-2-$PyPCl_4{\cdot}10.5H_2O$ ($C_{56}H_{75}N_8O_{10.5}Cl_4$): Found: C, 57.16; H, 6.94; N, 9.51; Cl, 11.77. Calculated: C,

57.10; H, 6.41; N, 9.51; Cl, 12.03%. H_2TnHex-2-PyPCl$_4$·11H_2O ($C_{64}H_{100}N_8O_{11}Cl_4$): Found: C, 59.19; H, 7.31; N, 8.61; Cl, 11.09. Calculated: C, 59.16; H, 7.751; N, 8.60; Cl, 10.91%. H_2TnOct-2-PyPCl$_4$·8.5H_2O ($C_{64}H_{111}N_8O_{8.5}Cl_4$): Found: C, 63.42; H, 7.90; N, 8.64; Cl, 10.86. Calculated: C, 63.29; H, 8.18; N, 8.20; Cl, 10.38%.

Mn^{III}T(alkyl)-2-PyP^{5+}. Metalation of the *N*-alkylated porphyrins was achieved as described previously for the methyl and ethyl compounds.[4,12] Metal incorporation became slower as the alkyl chains lengthened. Under the same conditions (20-fold excess metal, 25 °C, pH 12.3) it occurs almost instantaneously for methyl and ethyl, within minutes for n-propyl, in ≈30 minutes for n-butyl, in ≈1 hour with the n-hexyl, and took several hours at 100 °C for the n-octyl porphyrin. The formation of the Mn(II) porphyrin and its oxidation to Mn(III) were clearly distinguishable steps when the n-hexyl and n-octyl analogues were metalated. As was the case with the metal-free ligands, the PF_6^- salts of Mn(III) n-propyl, n-butyl, n-hexyl and n-octyl compounds were washed only with diethyl ether. Elemental analysis: Mn^{III}TnPr-2-PyPCl$_5$·11.5H_2O ($MnC_{52}H_{75}N_8O_{11.5}Cl_5$): Found: C, 50.90; H, 6.07; N, 9.27; Cl, 13.48. Calculated: C, 50.85; H, 6.16; N, 9.12; Cl, 14.43%. Mn^{III}TnBut-2-PyPCl$_5$·12.5H_2O ($MnC_{56}H_{85}N_8O_{12.5}Cl_5$): Found: C, 51.58; H, 6.33; N, 9.55; Cl, 15.53. Calculated: C, 51.64; H, 6.58; N, 8.60; Cl, 13.61%. Mn^{III}TnHex-2-PyPCl$_5$·10.5H_2O ($MnC_{64}H_{97}N_8O_{12.5}Cl_5$): Found: C, 55.64; H, 7.14; N, 8.23; Cl, 12.60. Calculated: C, 55.76; H, 7.09; N, 8.13; Cl, 12.86%. Mn^{III}TnOct-2-PyPCl$_5$·10H_2O·2.5NH_4Cl ($MnC_{64}H_{122}N_{10.5}O_{10}Cl_{7.5}$): Found: C, 53.56; H, 7.13; N, 9.12; Cl, 16.84. Calculated: C, 53.53; H, 7.60; N, 9.10; Cl, 16.46%.

Thin-layer chromatography

All ligands and their Mn(III) complexes were chromatographed on silica gel TLC plates using 1 : 1 : 8 KNO_3-saturated H_2O : H_2O : acetonitrile. The atropoisomers could not be separated for the methyl[19] and ethyl analogues,[2–4] they begin to separate for the n-propyl and n-butyl species and were clearly resolved with the n-hexyl and n-octyl compounds.

Uv/vis spectroscopy

The uv/vis spectra were taken on a Shimadzu UV-2501 PC spectrophotometer at 25 °C. The proton dissociation constants (pK_{a2}), were determined spectrophotometrically at 25 °C, at an ionic strength of 0.1 M (NaOH/$NaNO_3$), as previously described.[4]

Electrochemistry

Measurements were performed on a CH Instruments Model 600 Voltammetric Analyzer.[3,4] A three-electrode system in a small volume cell (0.5 to 3 mL), with a 3 mm diameter glassy carbon button working electrode (Bioanalytical Systems), plus the Ag/AgCl reference and Pt auxilliary electrodes was used. Solutions contained 0.05 M phosphate buffer, pH 7.8, 0.1 M NaCl, and 0.5 mM metalloporphyrin. The scan rates were 0.01–0.5 V s^{-1}, typically 0.1 V s^{-1}. The potentials were standardized against potassium ferrocyanide/ferricyanide[20] and/or against Mn^{III}TE-2-PyP^{5+}. All voltammograms were reversible.

Electrospray mass spectrometry

ESMS measurements were performed on a Micromass Quattro LC triple quadrupole mass spectrometer equipped with a pneumatically assisted electrostatic ion source operating at atmospheric pressure. Typically, the 0.5 mM 50% aqueous acetonitrile solutions of chloride salts of metal-free porphyrins or their Mn(III) complexes were introduced by loop injection into a stream of 50% aqueous acetonitrile flowing at 8 μL min^{-1}. Mass spectra were acquired in continuum mode, scanning from 100–500 *m*/*z* in 5 s, with cone voltages of 20 and 24 V. The mass scale was calibrated using polyethylene glycol.

Catalysis of $O_2^{\bullet-}$ dismutation

We have previously shown that the $O_2^{\bullet-}$/cytochrome c reduction assay gives the same catalytic rate constants as does pulse radiolysis for Mn^{III}TE-2-PyP^{5+}, {Mn^{III}BVDME}$_2$, {Mn^{III}-BV^{2-}}$_2$ and $MnCl_2$.[21] Therefore the convenient cytochrome c assay was used to characterize the series of Mn(III) *N*-alkylpyridylporphyrins. The xanthine/xanthine oxidase reaction was the source of $O_2^{\bullet-}$ and ferricytochrome c was used as the indicating scavenger for $O_2^{\bullet-}$.[22] The reduction of cytochrome c was followed at 550 nm. Assays were conducted at (25 ± 1) °C, in 0.05 M phosphate buffer, pH 7.8, 0.1 mM EDTA, in the presence and absence of 15 μg mL^{-1} of catalase. Rate constants for the reaction of metalloporphyrins with $O_2^{\bullet-}$ were based upon competition with 10 μM cytochrome c, $k_{cyt\ c} = 2.6 \times 10^5$ M^{-1} s^{-1} as described elsewhere.[21] The $O_2^{\bullet-}$ was produced at the rate of 1.2 μM per minute. Any possible interference through inhibition of the xanthine/xanthine oxidase reaction by the test compounds was examined by following the rate of urate accumulation at 295 nm in the absence of cytochrome c. No reoxidation of cytochrome c by the metalloporphyrins was observed.

Results

Thin layer chromatography

The increase in the length of the alkyl chains is accompanied by an increase in the lipophilicity of the compounds as indicated by the increase in the retention factor R_f (porphyrin path/solvent path) (Table 1, Fig. 1). The apparent lag that was observed in the case of shorter chains with Mn(III) complexes (Fig. 1B), is presumably due to their higher overall formal charge (+5 for the Mn(III) complexes, +4 for the ligand). As the chains lengthen, their contribution to the overall lipophilicity increases, and eventually the n-octyl porphyrin and its Mn(III) complex are more alike in R_f than are the methyl analogues.

Uv/vis spectroscopy

Molar absorptivities. The porphyrins obeyed the Beer–Lambert law from 10^{-7} to 10^{-5} M, and the uv/vis data are given in Table 2. As the length of the alkyl chains increased from methyl to n-butyl a red shift of the Soret absorption maximum was generally observed, as well as an increase in the molar absorptivities, and these effects plateau beyond the butyl compound. Such trends may be understood in terms of the interplay of porphyrin nucleus distortion (red shifts) and the electron-withdrawing (blue shifts) effect of the *N*-alkylpyridyl groups.[12,23]

Metalation behavior and proton dissociation constants. The rates of Mn^{2+} incorporation at pH ≈ 12.3 decreased with an increase in chain length. The same was found for the kinetics of Zn^{2+} and Cu^{2+} insertion into these compounds below pH 7, where the kinetics were first order in metal and porphyrin concentration.[24] Since the free-base porphyrin H_2P^{4+} reactants were mixtures of the four atropoisomers, each isomer has a similar metalation rate constant. As noted before for both water soluble and insoluble porphyrins, compounds with substituents in the *ortho* positions tend to metalate more slowly than derivatives with the same groups in the *meta* or *para* positions.[25–34]

The proton dissociation constants, K_{a2} and K_{a3} are defined as follows:

$$H_2P^{4+} \rightleftharpoons HP^{3+} + H^+ \ K_{a2} \qquad (1)$$

Table 1 Metal-centered redox potentials $E_{1/2}$, log k_{cat} for $O_2^{\bullet -}$ dismutation, and chromatographic R_f values

Porphyrin	R_f[a]	pK_{a2}[b]	$E_{1/2}$[c]/mV *vs.* NHE	log k_{cat}[d]
Mn^{III}TM-2-PyP^{5+}	0.09(0.13)	10.9	+220	7.79
Mn^{III}TE-2-PyP^{5+}	0.13(0.21)	10.9	+228	7.76
Mn^{III}TnPr-2-PyP^{5+}	0.20(0.31)	11.4	+238	7.38
Mn^{III}TnBut-2-PyP^{5+}	0.33(0.46)	11.7	+254	7.25
Mn^{III}TnHex-2-PyP^{5+}	0.57(0.63)	12.2	+314	7.48
Mn^{III}TnOct-2-PyP^{5+}	0.80(0.86)	13.2	+367	7.71

[a] R_f (compound path/solvent path) on silica gel TLC plates in 1 : 1 : 8 KNO_3-saturated H_2O : H_2O : acetonitrile. R_f for the metal-free porphyrins are in parentheses. [b] pK_{a2} determined at 25 °C ionic strength 0.10 M ($NaNO_3$/NaOH). [c] $E_{1/2}$ (±3 mV) determined in 0.05 M phosphate buffer (pH 7.8, 0.1 M NaCl). [d] k_{cat} (±20%) determined using the cytochrome c assay, in 0.05 M phosphate buffer, pH 7.8, at (25 ± 1) °C.

Table 2 Molar absorptivities of *meso*-tetrakis(*N*-alkylpyridinium-2-yl)porphyrin chlorides and their Mn(III) complexes

Porphyrin	λ_{nm} (log ε)[a]
H_2TM-2-PyP^{4+}	413.2(5.32); 510.4(4.13); 544.4(3.49); 581.4(3.72); 634.6(3.13)
H_2TE-2-PyP^{4+}	414(5.33); 511(4.20); 545(3.58); 582(3.80); 635(3.38)
H_2TnPr-2-PyP^{4+}	415(5.38); 511.5(4.24); 545(3.62); 583(3.84); 635(3.37)
H_2TnBut-2-PyP^{4+}	415(5.37); 511(4.24); 544(3.60); 583(3.84); 636(3.39)
H_2TnHex-2-PyP^{4+}	415.5(5.34); 510.5(4.24); 543(3.62); 584.5(3.84); 638(3.43)
H_2TnOct-2-PyP^{4+}	416.5(5.31); 510(4.25); 542(3.59); 585(3.82); 639.5(3.43)
Mn^{III}TM-2-PyP^{5+}	363.5(4.64); 411(4.27); 453.4(5.11); 499(3.66); 556(4.03); 782(3.15)
Mn^{III}TE-2-PyP^{5+}	363.5(4.68); 409(4.32); 454(5.14); 499(3.75); 558(4.08); 782(3.26)
Mn^{III}TnPr-2-Pyp^{5+}	363(4.70); 411(4.37); 454(5.21); 498(3.81); 559(4.12); 782(3.35)
Mn^{III}TnBut-2-PyP^{5+}	364(4.70); 410(4.35); 454(5.23); 498(3.83); 559(4.14); 781(3.33)
Mn^{III}TnHex-2-PyP^{5+}	364.5(4.70); 415(4.57); 454.5(5.21); 507(3.85); 560(4.12); 780(3.30)
Mn^{III}TnOct-2-PyP^{5+}	364(4.72); 414(4.44); 454.5(5.24); 500.5(3.84); 559.5(4.14); 781(3.25)

[a] The molar absorptivities were determined in water at room temperature.

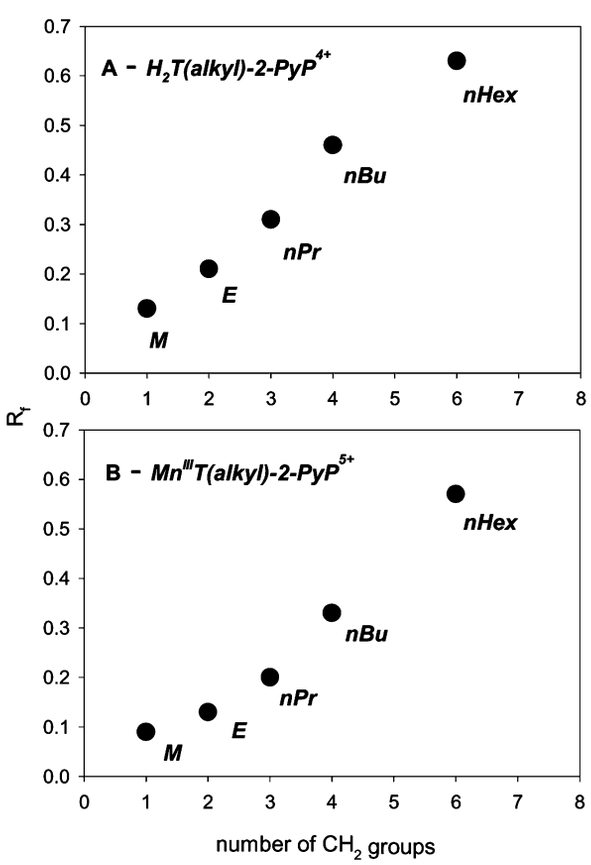

Fig. 1 The lipophilicity, R_f of H_2T(alkyl)-2-PyP^{4+} (A) and Mn^{III}-T(alkyl)-2-PyP^{5+} compounds (B) *vs.* the number of CH_2 groups.

$$H_3P^{5+} \rightleftharpoons H_2P^{4+} + H^+ \quad K_{a3} \qquad (2)$$

The pK_{a2} values for the *N*-alkylpyridyl series are given in Table 1. As the alkyl chains lengthen the porphyrins become less hydrated and the creation of charge (eqn. (1)) becomes less favorable, *i.e.* pK_{a2} increases (Fig. 2 insert). Fig. 2A shows the linear relationship between pK_{a2} and R_f.

Equilibrium constants pK_{a3} for reaction (2) are 1.8 for the *meta* H_2TM-3-PyP^{4+}, 1.4 for the *para* H_2TM-4-PyP^{4+}, and −0.9 for *ortho* H_2TM-2-PyP^{4+}.[4,25] While the *meta* and *para* *N*-methylpyridylporphyrins are mixtures of protonated H_3P^{5+} and H_4P^{6+} species in 1.0 M HCl, the *ortho* substituted H_2TM-2-PyP^{4+} to H_2TnOct-2-PyP^{4+} compounds remain as the unprotonated free base H_2P^{4+} in 1.0 M HCl and in 1.0 M HNO_3. With *ortho*, *meta* and *para* *N*-methylpyridylporphyrins pK_{a2} increases as pK_{a3} increases.

The half-lives for the acid and anion-catalyzed removal of zinc from Zn *N*-methylated derivatives[35] in 1.0 M HNO_3 were 89 s for the *meta*, 165 s for the *para*, and 19 hours for the *ortho* ZnTM-2-PyP^{4+}. No indication of zinc loss was found within a week for the ZnTnHex-2-PyP^{4+} compound.[36] Similar behavior is found in 1.0 M HCl, with $t_{1/2}$ ranging from 21 s for the *meta* methyl to 76 hours for ZnTnOct-2-PyP^{4+}.[24] In accord are the observations that when solid MnTnHex-2-PyP^{5+} was dissolved in 12 M HCl, the spectra did not change within 3 months, while over 50% of the Mn from Mn^{III}TM-2-PyP^{5+} species was lost within a month. In addition to porphyrin ring distortion,[29–32] the steric hindrance and solvation effects imposed by the progressively longer alkyl chains may also contribute to the differences in metalation/demetalation behavior.

Due to their high metal-centered redox potentials, the Mn(III) *meso*-tetrakis(*ortho* *N*-alkylpyridyl)porphyrins *in vivo* will be readily reduced with cell reductants such as ascorbic acid.[2,3,12] The reduced Mn(II) porphyrins will also be transiently formed in the catalysis of $O_2^{\bullet -}$ dismutation. Therefore, we also examined the behavior of the reduced and more biologically relevant Mn^{II}T(alkyl)-2-PyP^{4+} compounds. We compared the methyl, n-hexyl and n-octyl derivatives (6 μM) aerobically and anaerobically in the presence of a 70-fold excess of ascorbic acid (pH 7.8, 0.1 M tris buffer) and in the presence and absence of a 150-fold excess of EDTA. Under anaerobic conditions both Mn(II) porphyrins were stable to Mn loss and porphyrin decomposition inside 24 hours. Aerobically, ≈40% of Mn methyl but none of the Mn n-hexyl and n-octyl compounds underwent

Table 3 Electrospray mass spectrometry results for H_2T(alkyl)-2-PyP^{4+} compounds[a]

Species[b]	*m/z*					
	M	E	nPr	nBu	nHex	nOct
H_2P^{4+}/4	169	184	198	212	239	268
H_2P^{4+} + AN/4	180	194	208	222	250	
H_2P^{4+} + 2AN/4	190					
H_2P^{4+} − H^+/3	226	245	263	282	319	357
H_2P^{4+} − H^+ + AN/3	240	258	278			
H_2P^{4+} − H^+ + H_2O/3				288		
H_2P^{4+} − H^+ + Cl^-/2					496	
H_2P^{4+} − a^+/3		235	249	263	291	319
H_2P^{4+} − a^+ − H^+/2		352	374	394	436	
H_2P^{4+} − a^+ + H_2O/3			255			
H_2P^{4+} − $2a^+$/2			352	366		
H_2P^{4+} + H^+/5	136					
H_2P^{4+} + H^+ + AN/5	143					
H_2P^{4+} + H^+ + 2AN/5	152					
H_2P^{4+} + H^+ + $2Cl^-$/3					343	381
H_2P^{4+} + $2H^+$ + $2Cl^-$/4						286
H_2P^{4+} − $2H^+$/2	339	367	395	423	479	

[a] ≈0.5 mM solutions of H_2P^{4+} in 1 : 1 acetonitrile : water, 20 V cone voltage. [b] AN denotes acetonitrile and a is an alkyl group.

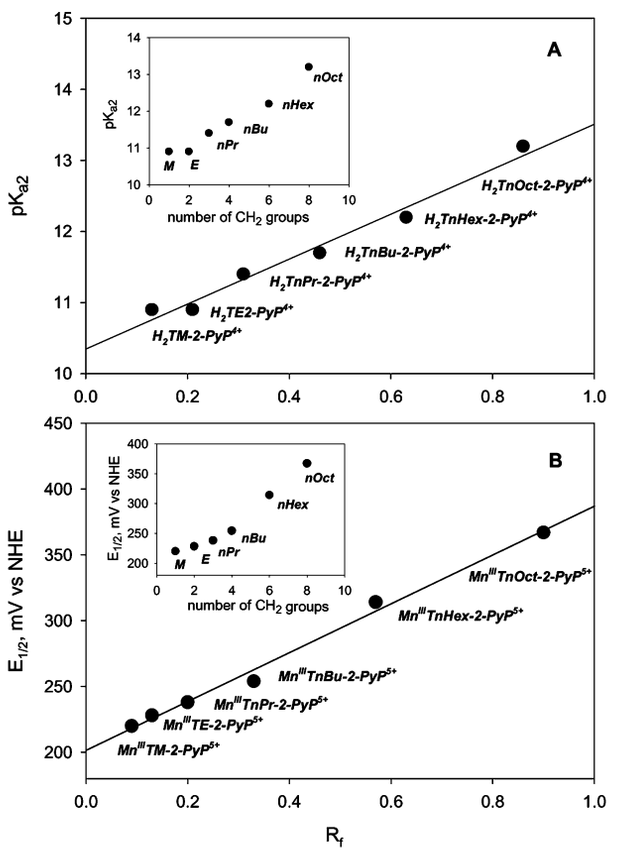

Fig. 2 Proton dissociation constants pK_{a2} of the metal-free porphyrins, H_2T(alkyl)-2-PyP^{4+} (A), and the metal-centered redox potentials $E_{1/2}$ for the Mn(III)/Mn(II) couple of $Mn^{III}T$(alkyl)-2-PyP^{5+} porphyrins (B) as a function of R_f. Inserts: pK_{a2} (Fig. 2A) and $E_{1/2}$ (Fig. 2B) *vs.* the number of CH_2 groups.

degradation within 125 min. The absorption spectral changes indicate that the degradation occurred through the Mn porphyrin catalyzed reduction of oxygen by ascorbate resulting in the formation of H_2O_2. The peroxide in turn causes porphyrin destruction. These observations are consistent with previous results which indicate that a more electron rich compound (Mn^{II}TM-2-PyP^{4+}) reduces O_2 faster than does a more electron deficient species (Mn^{II}TnOct-2-PyP^{4+}).[2,3] EDTA did not significantly influence porphyrin degradation or Mn loss.

Electrochemistry

Cyclic voltammetry of the Mn(III) porphyrins shows a reversible voltammogram that we ascribe to the Mn(III)/Mn(II) redox couple. The metal-centered redox potentials, $E_{1/2}$, are in Table 1 and the representative voltammograms of the $Mn^{III/II}$TE-2-$PyP^{5+/4+}$ and $Mn^{III/II}$TnHex-2-$PyP^{5+/4+}$ compounds are shown in the ESI, Fig. S1. Both lipophilicity (Fig. 1B) and $E_{1/2}$ (Fig. 2B, insert) increase exponentially with the number of CH_2 groups in the alkyl chains. Consequently, the increase in $E_{1/2}$ is a linear function of R_f (Fig. 2B).

Electrospray mass spectrometry

The ESMS proved to be a valuable tool for accessing the properties of the free base porphyrins and their Mn complexes whereby the impact of structure on solvation, ion-pairing, redox properties, protonation/deprotonation, dealkylation, and catalytic properties are clearly depicted.

H_2T(alkyl)-2-PyP^{4+}. The ESMS of the metal-free porphyrins obtained at the low cone voltage of 20 V showed dominant molecular ions assigned to H_2P^{4+}/4 and/or its mono-deprotonated analogue, H_2P^{4+} − H^+/3 (Table 3 and ESI, Figs. S2A–E). Negligible double deprotonation (H_2P^{4+} − $2H^+$/2) was noted. Only H_2TM-2-PyP^{4+} gave rise to a high-intensity H_2P^{4+} + H^+/5 peak.

The ESMS shows a pronounced decrease in solvation by acetonitrile as the alkyl chains lengthen. Compared to the base peak, the relative intensities of the mono-solvated molecular ions range from 40% for methyl, 15% for ethyl, and <10% for the higher analogues. Only with the n-hexyl and n-octyl porphyrins are small peaks (<5%) from ions associated with chloride found.

From methyl to n-butyl, the ratio of the molecular ion to mono-deprotonated ion peaks decreases. Thus, the base peak for methyl is that of the molecular ion, while the base peak for the n-propyl and n-butyl porphyrins is the mono-deprotonated ion. For the n-hexyl and n-octyl compounds roughly equal-intensity molecular ion (100%) and mono-deprotonated ion (98%) peaks are observed. The loss of one alkyl group (H_2P^{4+} − a^+/3) was noted for all derivatives (except for the methyl), and either no or negligible loss of a second alkyl group (H_2P^{4+} − $2a^+$/2) was found.

Mn^{III}T(alkyl)-2-PyP^{5+}. The ESMS of the Mn(III) complexes was done at a lower cone voltage (20 V) than in our previous study (30–58 V).[37] Therefore, less fragmentation occurs and more solvent-associated and ion-paired species could be observed (Table 4 and ESI, Figs. S3A–E). Solvation and ion pairing are more pronounced when compared with the metal-free ligands. The more lipophilic Mn(III) porphyrins are more easily desolvated in the electrospray ionization source. In accordance with our previous observations, the ESMS also clearly reflects the redox properties of these compounds.[37,38] The higher the $E_{1/2}$ the more reduced porphyrins are noted. Species solvated with acetonitrile or associated with chloride were observed with both Mn(III) and Mn(II) compounds. Two chlorides were associated only with Mn(III) porphyrins.

In the ESMS of the n-hexyl and n-octyl porphyrins we observed strong signals at *m/z* 337 and 375 that are assigned to compounds doubly reduced either at the metal ($Mn^{I}P^{3+}$/3) or at both the metal and porphyrin ring ($Mn^{II}P^{3+\bullet}$/3). Such doubly reduced manganese porphyrins should have a higher tendency to lose the metal, and indeed peaks for the metal-free species were found for the n-hexyl and n-octyl derivatives, while only traces of doubly reduced and demetalated species were found for n-butyl.

The ESMS behavior of Mn porphyrins changes sharply once the alkyl chains lengthen beyond butyl, as observed with

Table 4 Electrospray mass spectrometry for $Mn^{III}T(alkyl)\text{-}2\text{-}PyP^{5+}$ porphyrins[a]

Species[b]	*m/z*					
	M	E	nPr	nBu	nHex	nOct
$Mn^{III}P^{5+}/5$	146	157				
$Mn^{III}P^{5+}$ + AN/4	155	166	177	188		
$Mn^{III}P^{5+}$ + 2AN/5	163	174	185	196		
$Mn^{III}P^{5+}$ + 3AN/5	171	182	193	205		
$Mn^{III}P^{5+}$ + 4AN/5	179	190		213		
$Mn^{III}P^{5+}$ + 5AN/5	187	198				
$Mn^{III}P^{5+}$ + 6AN/5	195					
$Mn^{III}P^{5+}$ + H_2O/5	150					
$Mn^{III}P^{5+}$ + Cl^-/4	192	206		234	262	290
$Mn^{III}P^{5+}$ + $2Cl^-$/3	267	286	305	323	361	398
$Mn^{III}P^{5+}$ + Cl^- + AN/4	202	216	230	244	272	
$Mn^{III}P^{5+}$ − a/4			200			
$Mn^{III}P^{5+}$ − a + AN/4		200		221	242	
$Mn^{III}P^{5+}$ − a + Cl^-/3		264	279	293	321	349
$Mn^{III}P^{5+}$ − 2a/3		243	252	262		299
$Mn^{III}P^{5+}$ − 2a + AN/3				275	294	
$Mn^{II}P^{4+}/4$	183	197	211			281
$Mn^{II}P^{4+}$ + AN/4	193	207	221	235	263	
$Mn^{II}P^{4+}$ + 2AN/4	204					
$Mn^{II}P^{4+}$ + Cl^-/3	255	274	293	312	349	387
$Mn^{II}P^{4+}$ − a/3		253	266	281	309	337
$Mn^{III}P^{5+}$ − Mn^{3+} + H^+/3				281	319	357
$M^{II}P^{\bullet 3+}$/3 or $Mn^{I}P^{3+}$/3				294	337	375

[a] ≈0.5 mM solutions of $Mn^{III}P^{5+}$ in 1 : 1 acetonitrile : water, 20 V cone voltage. [b] AN denotes acetonitrile and a is an alkyl group.

corresponding metal-free analogues. No loss of methyl groups was detected.[37] As the chains lengthen up to butyl the loss of an alkyl group from Mn(III) and Mn(II) porphyrins becomes more pronounced and then the tendency decreases with n-hexyl and n-octyl. The same trend, but of lower intensity, was noted for the loss of two alkyl groups. The ratio of mono-chlorinated Mn(III) to mono-chlorinated Mn(II) species decreases from methyl to n-butyl and then increases up to n-octyl. Thus the base peak of the methyl and ethyl porphyrins relates to $Mn^{III}P^{5+}$ + Cl^-/4, while for the n-propyl and n-butyl derivatives it relates to $Mn^{II}P^{4+}$ + Cl^-/3. Yet, with the n-hexyl, the $Mn^{III}P^{5+}$ + Cl^-/4 and $Mn^{II}P^{4+}$ + Cl^-/3 peaks are both of 100% intensity, and the di-chlorinated species ($Mn^{III}P^{5+}$ + $2Cl^-$/3) is of 86% intensity. With the n-octyl analogue, the mono- and di-chlorinated species give rise to 100% $Mn^{III}P^{5+}$ + Cl^-/4 and 89% $Mn^{III}P^{5+}$ + $2Cl^-$/3 peaks, and the third most intense (59%) signal relates to $Mn^{II}P^{4+}$ + Cl^-/3. The lack of significant association of metal-free porphyrins with chloride observed here and elsewhere,[37] strongly supports the idea that chloride is bound to the metal. Furthermore, at the same cone voltage, the base peak of *ortho* $MnTM\text{-}2\text{-}PyP^{5+}$ is the mono-chlorinated species, which was only 35% for the *para* isomer. This suggests that the longer the chains, the more defined the cavity, which can hold up to two chloride ions, and the more stable is the Mn(III) state. While a species bearing two chlorides is hardly noted in $Mn^{III}TM\text{-}2\text{-}PyP^{5+}$, it is the second major peak in the ESMS of $Mn^{III}TnOct\text{-}2\text{-}PyP^{5+}$.

Catalysis of $O_2^{\bullet -}$ dismutation

None of the parent metal-free porphyrins exhibit any $O_2^{\bullet -}$ dismuting activity. All of the manganese compounds are potent catalysts of $O_2^{\bullet -}$ dismutation with log k_{cat} between 7.79 and 7.25. As shown in Table 1, log k_{cat} decreases from methyl to n-butyl and then increases, making n-octyl and methyl of comparable antioxidant potency.

Discussion

When designing metalloporphyrin SOD mimics we are aiming at approximating the redox properties of the enzyme active site. Superoxide dismutases catalyse the dismutation (disproportionation) of $O_2^{\bullet -}$ to H_2O_2 and O_2 at ≈ +300 V *vs.* NHE (pH 7.0).[39,40] This potential is roughly midway (+360 mV *vs.* NHE) between the potential for the reduction (+890 V *vs.* NHE)[41] and the oxidation of $O_2^{\bullet -}$ (−160 V *vs.* NHE)[41] thus providing an equal driving force for both half-reactions in the catalytic cycle. The $O_2^{\bullet -}$ dismutation by Cu,Zn–SOD occurs with catalytic rate constant, $k_{cat} = k_{red} = k_{ox} \simeq 2 \times 10^9\ M^{-1}\ s^{-1}$ ($\log k_{cat} \simeq 9.3$).[42–44]

We previously demonstrated a structure–activity relationship between log k_{cat} and the metal-centered $E_{1/2}$ of the Mn(III)/Mn(II) couple for a variety of water-soluble *meso* substituted porphyrins (Fig. 3A).[2–4] Electron-withdrawing substituents on the porphyrin ring shift $E_{1/2}$ towards more positive values resulting in higher values for k_{cat}.[2–4] Each 120 mV increase in $E_{1/2}$ gave a 10-fold increase in k_{cat},[4] consistent with the Marcus equation[45] for outer-sphere electron transfer reactions (Fig. 3A). The Marcus equation is valid as long as one of the two steps in the catalytic dismutation cycle

$$Mn^{III}P + O_2^{\bullet -} \rightleftharpoons Mn^{II}P^- + O_2,\ k_{red} \qquad (3)$$

$$Mn^{II}P^- + O_2^{\bullet -} + 2H^+ \rightleftharpoons Mn^{III}P + H_2O_2,\ k_{ox} \qquad (4)$$

is rate-limiting (in our case eqn. (3)). For simplicty, porphyrins having Mn in its +3 state are written as neutral species in eqn. (3) and (4).

On the basis of such structure–activity relationships, the *ortho* isomers of Mn(III) *meso*-tetrakis *N*-methyl- and *N*-ethylpyridylporphyrins were tested and proved to be potent catalysts of $O_2^{\bullet -}$ dismutation. Their log k_{cat} values are 7.79 and 7.76 and they operate at potentials (+220 and +228 V) similar to the potential of the enzyme itself. These two metalloporphyrins also exhibit protection in *in vivo* models of oxidative stress injuries.[14–17] We have now extended our work to a series of $Mn^{III}T(alkyl)\text{-}2\text{-}PyP^{5+}$ compounds where alkyl is methyl, ethyl, n-propyl, n-butyl, n-hexyl, and n-octyl (Scheme 1). The significant differences in lipophilicity along the series (Fig. 1A), with retention of catalytic potency (Table 1), might lead to favorably selective subcellular distributions of these new $Mn^{III}T(alkyl)\text{-}2\text{-}PyP^{5+}$ compounds and hence broaden their utility.

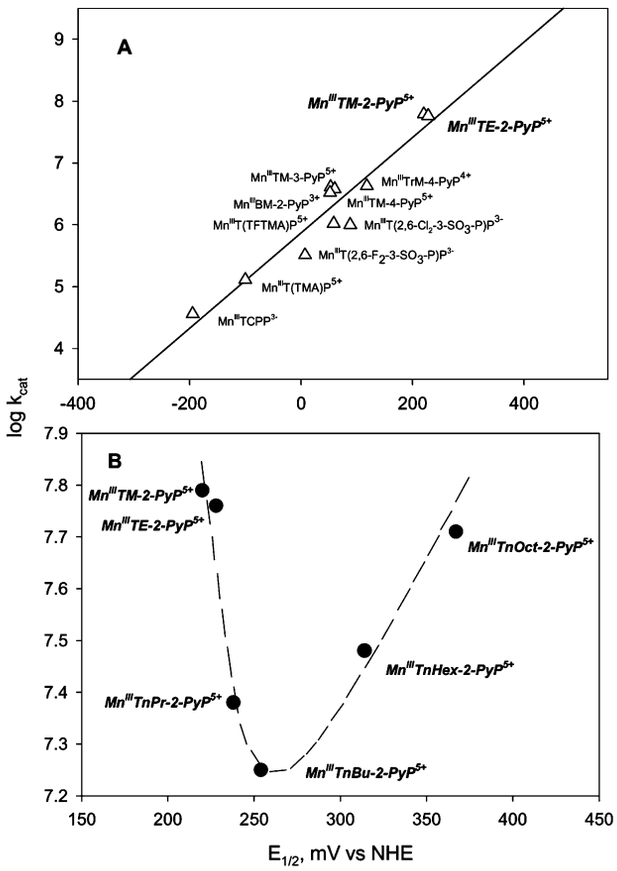

Fig. 3 The reactivity of water-soluble Mn(III) porphyrins (A) (ref. 4) and $Mn^{III}T(alkyl)\text{-}2\text{-}PyP^{5+}$ porphyrins (B) as catalysts for $O_2^{\bullet-}$ dismutation, expressed in terms of log k_{cat} *vs.* $E_{1/2}$.

$E_{1/2}$ *vs.* pK_{a2}

We did not expect a profound change in $E_{1/2}$ along the series based on the fact that the increase in alkyl chain length from methyl to n-hexyl is without effect on the basicity of alkylamines.[46] However, we found that the metal-centered redox potentials varied from +220 mV for methyl to +367 mV (*vs.* NHE) for the n-octyl compound. Such an increase in $E_{1/2}$ may originate from progressively unshielded positive charges at pyridyl nitrogens which would then exert a stronger electron-withdrawing effect on the coordinated Mn as the compounds increase in lipophilicity. This reasoning is supported by the ESMS data (Table 4 and ESI, Figs. S3A–E) which show that the susceptibility to desolvation is accompanied by a greater preponderance of reduced Mn(II) porphyrin ions as the alkyl chains of the Mn complexes lengthen. We have previously reported[4] that mainly electronic effects determine the relation between the pK_a of the metal-free porphyrin and the $E_{1/2}$ of the corresponding metal complex such that the decrease in pK_{a3} is accompanied by a linear increase in $E_{1/2}$ (Fig. 4, insert). However, as the compounds become increasingly more lipophilic, the lack of solvation disfavors creation of charge (higher pK_{a2} values), while the electron-withdrawing effects of the positively charged pyridyl nitrogens are enhanced. Thus the electronic pK_{a2} effects are overcome by solvation/steric effects resulting in an inverted trend, *i.e.* the $E_{1/2}$ now increases in a linear fashion with an increase in pK_{a2} (Fig. 4).

Log k_{cat} *vs.* $E_{1/2}$

Based on previously established structure–activity relationships for water-soluble Mn(III) porphyrins,[4] we expected the 147 mV increase in $E_{1/2}$ to be accompanied by a ≈12-fold increase in k_{cat} (Fig. 3A).[4] We actually found that k_{cat} decreased from methyl to n-butyl, and then increased by the same factor of ≈3 to n-octyl (Table 1, Fig. 3B). One explanation is that the Mn porphyrins are solvated to different extents, as indicated by the ESMS data, and this in turn affects the magnitude of k_{cat}. The trend in k_{cat} may also be influenced by the electrostatic/steric effects originating from the shielding of the single positive charge on the

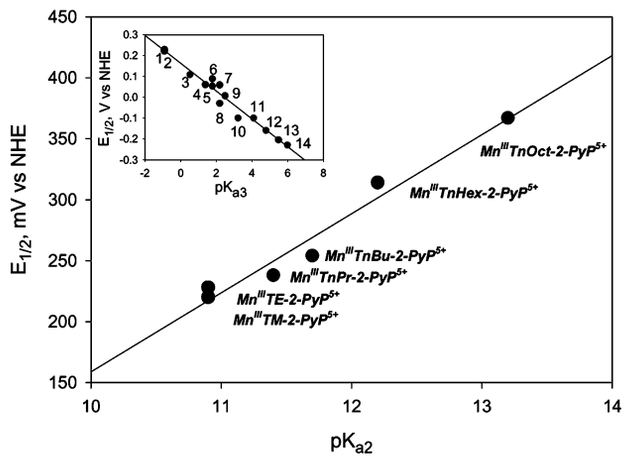

Fig. 4 $E_{1/2}$ for the Mn(III)/Mn(II) couple of $Mn^{III}T(alkyl)\text{-}2\text{-}PyP^{5+}$ porphyrins *vs.* pK_{a2} of the corresponding metal-free ligands. Insert: $E_{1/2}$ of water-soluble Mn(III) porphyrins *vs.* pK_{a3} (data from ref. 4); $Mn^{III}TE\text{-}2\text{-}PyP^{5+}$ (1), $MnTM\text{-}2\text{-}PyP^{5+}$ (2), $MnPTrM\text{-}2\text{-}PyP^{4+}$ (3), $Mn^{III}TM\text{-}4\text{-}PyP^{5+}$ (4), $Mn^{III}TM\text{-}3\text{-}PyP^{5+}$ (5), $Mn^{III}T(2,6\text{-}Cl_2\text{-}3\text{-}SO_3\text{-}P)P^{3-}$ (6), $Mn^{III}T(TFTMA)P^{5+}$ (7), $Mn^{III}T(\alpha\alpha\alpha\alpha\text{-}2\text{-}MINP)P^{5+}$ (8), $Mn^{III}T(2,6\text{-}F_2\text{-}3\text{-}SO_3\text{-}P)P^{3-}$ (9), $Mn^{III}T(2,4,6\text{-}Me_3\text{-}3,5\text{-}(SO_3)_2\text{-}P)P^{7-}$ (10), $Mn^{III}(TMA)P^{5+}$ (11), $MnTSPP^{3-}$ (12), $MnTCPP^{3-}$ (13), $Mn^{III}hematoP^{-}$ (14).

Mn(III) center. Thus the difference in the magnitude of lipophilicity between the metal-free ligands (formally +4) and the Mn(III) complexes (formally +5) becomes less noticeable as the alkyl chains get longer (Table 1). These H_2P^{4+} compounds of formal +4 charge behave in solution kinetically as +1.6 to +1.8 electrolytes.[24] From methyl to n-butyl, log k_{cat} decreases almost linearly (Fig. 3B, insert). Due to the exponential increase in $E_{1/2}$ along the series of Mn porphyrins (Fig. 2B, insert), the unfavorable electrostatic/steric effects are in part opposed and finally overcome by the progressively more favorable redox potentials that originate from increased desolvation (lipophilicity). Consequently, the very lipophilic n-octyl compound is essentially as potent a SOD mimic as the less lipophilic methyl and ethyl derivatives.

Regan *et al.*[47] were able to uncouple the steric and solvation effects in reactions of chloride ions with methyl- and *tert*-butyl-substituted chloroacetonitrile, and showed that both were of comparable magnitudes. Similarly, the reactivity of *N*-alkylpyridylporphyrins are the result of the interplay of electronic, steric and solvation effects, the latter dominating with the more lipophilic members of the series.

Recent findings indicate that biologically relevant reactions, other than $O_2^{\bullet-}$ dismutation, can occur at the metal center in Mn porphyrins.[2,3,5,7,8,48–52] The same has been reported for the enzyme active site,[53–57] thus raising the complexity of the free radical chemistry and biology of the enzymes and their mimics. Reactive oxygen and nitrogen species are involved in direct damage of key biological targets such as nucleic acids, proteins and fatty acids, and there is an increasing amount of evidence that such species are also involved in the modulation of signaling processes.[14,58,59] Thus, it is important to understand the mechanisms of action of Mn porphyrins and related compounds. Based on the electrostatic, steric, solvation, and lipophilic effects observed in this study, we expect the members of *N*-alkylpyridyl series to differ one from another in *in vivo* models of oxidative stress injuries with respect to their specificity towards reactive oxygen and nitrogen species as well as with regard to their pharmacokinetics. Such work is in progress.

Acknowledgements

The authors are grateful for financial support from a Duke Comprehensive Cancer Center Award, NCI P30CA14236, from the Christopher Reeve Paralysis Foundation, BA1–0103–1, and from Aeolus/Incara Pharmaceuticals, Research Triangle Park, NC. P. H. was supported by the CSTEA/NASA grant at Howard University.

References

1 (*a*) R. F. Pasternack, A. Banth, J. M. Pasternack and C. S. Johnson, *J. Inorg. Biochem.*, 1981, **15**, 261; (*b*) R. F. Pasternack and B. J. Halliwell, *J. Am. Chem. Soc.*, 1979, **101**, 1026.
2 I. Batinić-Haberle, *Methods Enzymol.*, 2002, **349**, 223.
3 I. Spasojević and I. Batinić-Haberle, *Inorg. Chim. Acta*, 2001, **317**, 230.
4 I. Batinić-Haberle, I. Spasojević, P. Hambright, L. Benov, A. L. Crumbliss and I. Fridovich, *Inorg. Chem.*, 1999, **38**, 4011.
5 G. Ferrer-Sueta, I. Batinić-Haberle, I. Spasojević, I. Fridovich and R. Radi, *Chem. Res. Toxicol.*, 1999, **12**, 42.
6 R. Kachadourian, I. Batinić-Haberle and I. Fridovich, *Inorg. Chem.*, 1999, **38**, 391.
7 J. Lee, J. A. Hunt and J. T. Groves, *J. Am. Chem. Soc.*, 1998, **120**, 6053.
8 J. P. Crow, *Arch. Biochem. Biophys.*, 1999, **371**, 41.
9 M. Patel and B. J. Day, *Trends Pharmacol.*, 1999, **20**, 359.
10 (*a*) K. Aston, N. Rath, A. Naik, U. Slomczynska, O. F. Schall and D. P. Riley, *Inorg. Chem.*, 2001, **40**, 1779; (*b*) S. Cuzzocrea, E. Mazzon, L. Dugo, A. P. Caputi, K. Aston, D. P. Riley and D. Salvemini, *Br. J. Pharmacol.*, 2001, **132**, 19.
11 (*a*) S. Melov, J. Ravenscroft, S. Malik, M. S. Gill, D. W. Walker, P. E. Clayton, D. C. Wallace, B. Malfroy, S. R. Doctrow and G. J. Lithgow, *Science*, 2000, **289**, 1567; (*b*) K. Baker, C. Bucay Marcus, K. Huffman, H. Kruk, B. Malfroy and S. R. Doctrow, *J. Pharmacol. Exp. Ther.*, 1998, **284**, 215.
12 I. Batinić-Haberle, L. Benov, I. Spasojević and I. Fridovich, *J. Biol. Chem.*, 1998, **273**, 24521.
13 I. Spasojević, R. Menzeleev, P. S. White and I. Fridovich, *Inorg. Chem.*, 2002, submitted.
14 G. B. Mackensen, M. Patel, H. Sheng, C. C. Calvi, I. Batinić-Haberle, B. J. Day, L. P. Liang, I. Fridovich, J. D. Crapo, R. D. Pearlstein and D. S. Warner, *J. Neurosci.*, 2001, **21**, 4582.
15 J. D. Piganelli, S. C. Flores, C. Cruz, J. Koepp, I. Batinić-Haberle, J. Crapo, B. J. Day, R. Kachadourian, R. Young, B. Bradley and K. Haskins, *Diabetes*, 2002, **51**, 347.
16 M. Aslan, T. M. Ryan, B. Adler, T. M. Townes, D. A. Parks, J. A. Thompson, A. Tousson, M. T. Gladwin, M. M. Tarpey, M. R. P. Patel, I. Batinić-Haberle, C. R. White and B. A. Freeman, *Proc. Natl. Acad. Sci. USA*, 2001, **98**, 15215.
17 (*a*) I. Batinić-Haberle, I. Spasojević, I. Fridovich, M. S. Anscher and Ž. Vujaskovic, *Proceedings of the 43rd Annual Meeting of American Society for Therapeutics in Radiation Oncology*, San Francisco, 2001, 235–236; (*b*) Z. Vujašković, I. Batinić-Haberle, I. Spasojević, T. V. Samulski, M. W. Dewhirst and M. S. Anscher, *Annual Meeting of Radiation Research Society*, San Juan, Puerto Rico, 2001; (*c*) Ž. Vujašković, I. Batinić-Haberle, I. Spasojević, I. Fridovich, M. S. Anscher and M. W. Dewhirst, *Free Radicals Biol. Med.*, 2001, S128.
18 W. R. Waud, F. O. Brady, R. D. Wiley and K. V. Rajagopalan, *Arch. Biochem. Biophys.*, 1975, **19**, 695.
19 T. Kaufmann, T. B. Shamsai, R. S. Lu, R. Bau and G. M. Miskelly, *Inorg. Chem.*, 1995, **34**, 5073.
20 I. M. Kolthof and W. J. Tomsicek, *J. Phys. Chem.*, 1935, **39**, 945.
21 I. Batinić-Haberle, I. Spasojević, R. D. Stevens, P. Hambright, A. N. Thorpe, J. Grodkowski, P. Neta and I. Fridovich, *Inorg. Chem.*, 2001, **40**, 726.
22 J. M. McCord and I. Fridovich, *J. Biol. Chem.*, 1969, **244**, 6049.
23 I. Batinić-Haberle, S. I. Liochev, I. Spasojević and I. Fridovich, *Arch. Biochem. Biophys.*, 1997, **343**, 225.
24 P. Hambright, I. Spasojević, I. Fridovich and I. Batinić-Haberle, in preparation.
25 P. Hambright, *Water-Soluble Metalloporphyrins*, in *The Porphyrin Handbook*, K. M. Kadish, K. M. Smith, R. Guillard, Eds. Academic Press, N. Y., 2000, ch. 18.
26 T. P. G. Sutter and P. Hambright, *J. Coord. Chem.*, 1993, **30**, 317.
27 L. R. Robinson and P. Hambright, *Inorg. Chem.*, 1992, **31**, 652.
28 J. B. Reid and P. Hambright, *Inorg. Chem.*, 1977, **16**, 968.
29 M. Inamo, N. Kamiya, Y. Inada, M. Nomura and S. Funahashi, *Inorg. Chem.*, 2001, **40**, 5636.
30 P. B. Chock and P. Hambright, *J. Am. Chem. Soc.*, 1974, **96**, 3123.
31 S. Funahashi, Y. Inada and M. Inamo, *Anal. Sci.*, 2001, **17**, 917.
32 T. P. G. Sutter, R. Rahimi, P. Hambright, J. Bommer, M. Kumar and P. Neta, *J. Chem. Soc., Faraday Trans.*, 1993, **84**, 495.
33 B. Cheng, O. Q. Munro, H. M. Marques and W. R. Scheidt, *J. Am. Chem. Soc.*, 1997, **119**, 10732.
34 R. F. Pasternack, N. Sutin and D. H. Turner, *J. Am. Chem. Soc.*, 1976, **98**, 1908.
35 P. Hambright, T. Gore and M. Burton, *Inorg. Chem.*, 1976, **15**, 2314.
36 J. Davilla, A. Harriman, M.-G. Richoux and L. R. Milgrom, *J. Chem. Soc., Chem. Commun.*, 1987, 525.
37 I. Batinić-Haberle, R. D. Stevens and I. Fridovich, *J. Porphyrins Phthalocyanines*, 2000, **4**, 217.
38 R. Kachadourian, N. Srinivasan, C. A. Haney and R. D. Stevens, *J. Porphyrins Phthalocyanines*, 2001, **5**, 507.
39 C. K. Vance and A.-F. Miller, *Biochemistry*, 2001, **40**, 13079.
40 (*a*) G. D. Lawrence and D. T. Sawyer, *Biochemistry*, 1979, **18**, 3045; (*b*) W. C. Barrette, Jr., D. T. Sawyer, J. A. Free and K. Asada, *Biochemistry*, 1983, **22**, 624.
41 P. M. Wood, *J. Biochem.*, 1988, **253**, 287.
42 C. K. Vance and A.-F. Miller, *J. Am. Chem. Soc.*, 1998, **120**, 461.
43 R. M. Ellerby, D. E. Cabelli, J. A. Graden and J. S. Valentine, *J. Am. Chem. Soc.*, 1996, **118**, 6556.
44 D. Klug-Roth, I. Fridovich and J. Rabani, *J. Am. Chem. Soc.*, 1973, **95**, 2786.
45 R. A. Marcus, *Annu. Rev. Phys. Chem.*, 1964, **15**, 155.
46 *CRC Handbook of Chemistry and Physics*, D. R. Lide, Editor-in-Chief, 74th Edition, CRC Press, Boca Raton, 1993–1994.
47 C. K. Regan, S. L. Craig and J. I. Brauman, *Science*, 2002, **295**, 2245.
48 I. Spasojević, I. Batinić-Haberle and I. Fridovich, *Nitric Oxide: Biol. Chem.*, 2000, **4**, 526.
49 R. Shimanovich and J. T. Groves, *Arch. Biochem. Biophys.*, 2001, **387**, 307.
50 N. Jin, J. L. Bourassa, S. C. Tizio and J. T. Groves, *Angew. Chem., Int. Ed.*, 2000, **39**, 3849.
51 H. Zhang, J. Joseph, M. Gurney, D. Becker and B. Kalyanaraman, *J. Biol. Chem.*, 2002, **277**, 1013.
52 N. Motohashi and Y. Saito, *Chem. Pharm. Bull.*, 1995, **43**, 505.
53 C. Quijano, D. Hernandez-Saavedra, L. Castro, J. M. McCord, B. A. Freeman and R. Radi, *J. Biol. Chem.*, 2001, **276**, 11631.
54 (*a*) S. L. Jewet, A. M. Rocklin, M. Ghanevati, J. M. Abel and J. A. Marach, *Free Radicals Biol. Med.*, 1999, **26**, 905; (*b*) S. P. A. Goss, R. J. Singh and B. Kalyanaraman, *J. Biol. Chem.*, 1999, **274**, 28233; (*c*) S. I. Liochev and I. Fridovich, *Free Radicals Biol. Med.*, 199, **27**, 1444.
55 (*a*) A. G. Estevez, J. P. Crow, J. B. Sampson, L. Reither, J. Zhuang, G. J. Richardson, M. M. Tarpey, L. Barbeito and J. S. Beckman, *Science*, 1999, **286**, 2498; (*b*) S. I. Liochev and I. Fridovich, *J. Biol. Chem.*, 2001, **276**, 35253.
56 S. I. Liochev and I. Fridovich, *J. Biol. Chem.*, 2000, **275**, 38482.
57 E. D. Coulter, J. P. Emerson, D. M. Kurtz, Jr. and D. E. Cabelli, *J. Am. Chem. Soc.*, 2000, **122**, 11555.
58 B. M. Matata and M. Galinanes, *J. Biol. Chem.*, 2002, **277**, 2330.
59 (*a*) Ž. Vujašković, I. Batinić-Haberle, M. S. Anscher, Z. N. Rabbani, T. V. Samulski, K. Amin, M. W. Dewhirst and Z. Haroon, *Proceedings of the 43rd Annual Meeting of American Society for Therapeutics in Radiation Oncology*, San Francisco, 2001, pp. 88–89; (*b*) Ž. Vujašković, I. Batinić-Haberle, Z. N. Rabbani, Q.-F. Feng, S. K. Kang, I. Spasojević, T. V. Samulski, I. Fridovich, M. W. Dewhirst and M. S. Anscher, *Free Radicals Biol. Med.*, in press.